Aquacultural Engineering 26 (2002) 129–147
aquacultural engineering
www.elsevier.com/locate/aqua-online

Effect of speed on Taiwanese paddlewheel aeration

Eric L. Peterson *, Margaret B. Walker

School of Engineering, James Cook University, Townsville 4811, Australia

Received 26 July 2001; accepted 3 April 2002

Abstract

Aerators are generally used in Australian aquaculture ponds day and night at full speed without regulation. This situation is untenable in view of climate change, as energy conservation becomes an essential issue for all industries, including aquaculture. Variable speed performance curves were developed for the paddlewheel aerators that have been employed on Australian marine aquaculture ponds so that speed may be actively adjusted to match pond water quality requirements. Results show that speed of rotation is a significant factor effecting the performance of a paddlewheel aerator. Of particular note was the observation of backsplashing when kinetic energy (pumping head) was greater than the radius of a paddlewheel. The process of backsplashing is readily identified when whitewater is seen flying above a paddlewheel. It is hypothesised that backsplashing dilutes the oxygen-starved water entering a paddlewheel, thereby degrading the operational efficiency. Backsplash breakpoint speed is related to paddlewheel diameter. Aerator users can reduce backsplash by changing mechanical gearboxes or using a variable frequency drive (VFD inverter).

Keywords: Aeration; Paddlewheel; Oxygen transfer; Energy conservation

1. Introduction

Aquaculture ponds require artificial aeration when stock biomass exceeds the natural re-aeration rate delivered by wind, photosynthesis, and water exchange

* Corresponding author. Present address: Aquaculture Department, School of Engineering, James Cook University, Townsville 48811, Australia. Tel.: + 61-7-4781-5346; fax: + 61-7-4781-4585.

E-mail address: eric.peterson@jcu.edu.au (E.L. Peterson).

0144-8609/02/$ - see front matter
PII: S0144-8609(02)00009-2

(Boyd, 1998). Aeration consumed 70–80% of the power load found in three energy audits of Australian aquaculture farms (Peterson and Patterson, 2000), generally confirmed by a review of intensive shrimp culture practices overseas (Fast, 1992). Australian practices are typically intensive, with a reliance on mechanical aerators, which are usually Taiwanese paddlewheels (Peterson, 1997).

The dissolved oxygen (DO) capacity of water is limited to a few mg/l, in contrast to the 21% oxygen content of air. Natural re-aeration at the surface of a water body is limited by molecular diffusion, unless turbulence and extended surface area are provide by wind, waves, or currents. Mechanical aeration allows much higher biomass concentrations than could be supported in a natural waterway. Aerators serve as the 'lungs' of an intensive aquaculture pond: pumping oxygen into the water column; and stripping carbon dioxide out (Peterson and Pearson, 2000). Photosynthetic plankton actively generates oxygen and creates biomass at the expense of carbon dioxide when sunlight and nutrients are available. Strong sunlight may result in supersaturated pond oxygen levels. Mechanical aerators only enhance the passive diffusion of oxygen down-gradient, and so they will strip oxygen out of a supersaturated pond. It may be warranted to switch mechanical aerators off during daylight, but they are important for circulation (Rogers, 1989; Busch, 1980; Fast and Boyd, 1992). Boyd (1998) geared the speed of a specially designed spiralled paddlewheel, finding greater efficiencies at low speeds.

In the present paper it is shown that the conventional aerators mass-produced in Taiwan and China can be operated at reduced speed to achieve better efficiency. Furthermore the present paper suggests that the process of backsplashing should be generally avoided when designing and operating paddlewheel aerators. Backsplashing is readily identified when whitewater is seen flying above a paddlewheel. It is hypothesised that backsplash droplets fall into the intake of the machine, creating a condition of hydraulic short-circuiting. Hydraulic short-circuiting may be expected to reduce the gas-transfer capacity or increase the power requirement of an aerator.

Lewis and Whitman (1924) developed the two-film theory to model mass transfer of dissolved substances existing in a state of quasi-equilibrium at the interface between two phases, which can be applied to air and water. They modelled mass transfer at the interface with vapour velocity, k_G, in the gas phase and solute velocity, k_L, in the liquid phase. The bottleneck is effectively on the aqueous side of the interface because gas molecule velocities are many orders of magnitude higher. Eq. (1) gives solute transfer flux J^* per unit of interface area.

$$J^* = k_L(C_b - C_s^*) \tag{1}$$

The solute concentration, C, is spatially variable with distance from the interface. C_b denotes the concentration throughout the bulk of the water column, whereas C_s^* denotes the saturation condition found at the outer boundary of the liquid phase.

ASCE (1993) established a standard for measurement of oxygen transfer by full-scale aeration systems used in the wastewater treatment industry. The contact area of the two-film interface is not practically determinable, but the product of mass transfer velocity and area, k_La (lower case k), is readily measured from the product of the time-constant of re-aeration, K_La (upper case K), and the volume of the experimental reactor, Vol. The standardised mass transfer measurement, K_La_{20} may be taken from the product of the observed K_La, and a temperature correction factor, $\theta^{(20°C-T)}$, where the base θ may have a value of 1.024. Standard oxygen transfer rate (SOTR) may then be determined from the volume of water in the test tank using Eq. (2) to represent the maximum oxygen transfer rate,

$$\mathrm{SOTR} = k_La_{20}C^*_{20} = K_La_{20}C^*_{20}\mathrm{Vol} \tag{2}$$

Standard aeration efficiency (SAE) may be expressed as $\mathrm{kg_{DO}/kW\,h_{electricity}}$ to represent the aeration effect per unit of energy use. SAE is determined with Eq. (3),

$$\mathrm{SAE} = \mathrm{SOTR/Power\ input} \tag{3}$$

Actual aeration effect varies with actual DO-deficit ($C_b - C^*_s$), and will be negative whenever pond water is supersaturated.

Boyd (1998) reviewed the ASCE standard method and tabulated the performance ratings of various types of mechanical aerators used in aquaculture ponds. Paddlewheels, propeller-aspirators, vertical splashers and pump sprayers were generally found to have SAE ratings over 1 kg O_2/kW h. The spiral paddlewheel design promoted by Boyd as having an SAE of 3-kgO_2/kW h was much more efficient than the Taiwanese paddlewheels that dominate the world market.

Increasing salinity tends to reduce surface tension, causing smaller diameter bubbles and droplets. This provides a greater interface surface area, a, and so k_La is expected to increase with salinity. Fast et al. (1999) measured the effect of salinity on the oxygen transfer of paddlewheels, finding that increasing dissolved solids up to 11 ppt effectively enhances mass transfer about 50% above the freshwater condition.

Gnezdiloff (1999) found the efficiency of a typical Taiwanese paddlewheel might increase when speed was reduced below the nominal 100 rpm. Peterson and Patterson (1999, 2000) explained that operation at faster speed results in backsplashing. Linear regression curves for the paddlewheel tested by Boyd (1998) were developed for 610 and 910 mm diameter spiral wheels with speeds in the range of 75–125 rpm, which may have been entirely above the speed of backsplashing, and missed potentially interesting effects at or below backsplashing breakpoint speed.

In this paper we document experiments aiming to determine the relationship between speed and performance for the typical paddlewheel designs in the Eastern Hemisphere. These data provide aquaculturalists an indication if performance varies between manufacturers, and how they will behave if speed controlled with a variable frequency inverter.

2. Methods

Three different manufacturers provided paddlewheel aerators. Their identities will not be revealed in the present paper, because this was a scientific investigation, not a marketing exercise. The identifiers ‘A’, ‘B’, and ‘C’ distinguish them.

Performance testing of aerators utilised a concrete basin filled with clean water and free from sediment oxygen demand. An oxygen scavenger chemical was weighed and mixed into the basin until DO was below 10% of saturation. In each experiment, the aerator was first operated at low speed as required to mix the scavenger agent into the water column. Then aeration behaviour could be tested by increasing speed to the level of interest and finally logging DO levels in the tank until it surpassed 70% saturation.

Paddlewheel speed was controlled by adjusting electric power frequency with a 3 phase Vacon CXS inverter. The aerators each included a 0.75 kW (1 hp) 4-pole motor with 14:1 worm-drive gearbox driving two paddlewheels at 103 rpm. This was a very typical Taiwanese paddlewheel design, with blue plastic moulded material used for buoyant pontoons and motor/gearbox cover. Wheels were yellow plastic, 680 mm diameter tip-to-tip, comprised of six constituent paddles. Paddle-blades were 200 mm wide with 0.03 m^2 face area, less perforation patterns that varied in diameter and number between manufacturers.

Three phase electric power kW was determined in accordance with Eq. (4),

$$\mathrm{kW} = \sqrt{3} \times (\mathrm{Amps}) \times (\mathrm{Volts}) \times (\mathrm{power\_factor}) \times 10^{-3}\ \mathrm{kW/W} \quad (4)$$

Electric power measurements should not be based upon an assumed power factor, as this may vary within any electricity network. Power factor was completely accounted for with a direct connect digital polyphase meter ZMB120T244 by Landis and Gyr. It was generally found that kW is proportional to rpm^n, where exponent n was about 1.6, varying as detailed in Fig. 1. The speed of paddlewheel operation was determined by the frequency of alternating current (A/C) electric

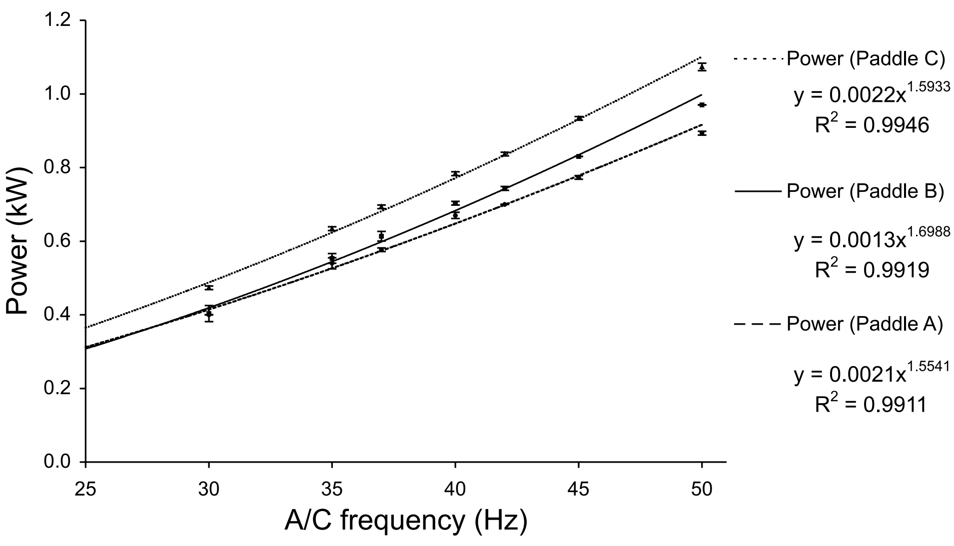

Fig. 1. Aerial view of the basin used for aerator testing. A, B, C, and D (right side) mark the alternative locations of oxygen probe tested during a pilot study as required by the testing standard.

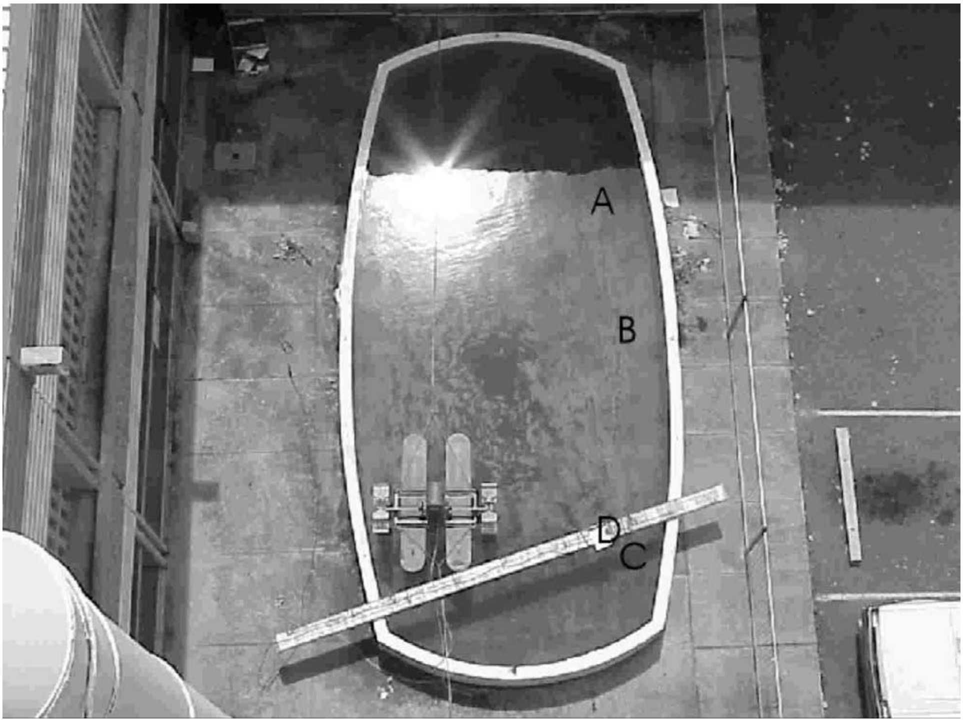

Fig. 2. Electric power demand of aerators.

power, the number of motor poles, and the gearbox ratio. Assuming motors slip 50 rpm at nominal full load, and that slip varies in proportion to partial loads, Eq. (5) quantifies the relationship between electric power supply $Hz_{A/C}$ and $rpm_{paddlewheel}$.

$$rpm_{paddlewheel} = \frac{Hz_{A/C} \times 60\ s/min \times 2}{motor\text{-}poles \times Gearing} - \frac{slip_{nominal}}{Gearing} \times \left(\frac{Hz_{A/C}}{Hz_{nominal}}\right)^{n} \quad (5)$$

Gearing is typically 14, $slip_{nominal}$ is typically 50 rpm and $Hz_{nominal}$ is either 50 or 60 Hz. SAE was based upon electric power consumption, rather than mechanical energy delivered to the paddles. This more fairly represents the cost of operation, but yields figures that are numerically lower than those normally advertised.

The test basin was 8.85 m long and 4.173 m at the greatest width, oval shaped as illustrated in Fig. 2. Spatial replicate tests were carried out with the aerators always situated as shown. Our oxygen transfer measurements were generally in accordance with the ASCE/ANSI 2-91 standard (1993), except only one DO probe was used. Data were acquired at 10 s intervals, providing a high-resolution representation of DO levels as water circulated around the testing basin. Fig. 3 illustrates the density of data, where bumps are the tracks of individual parcels of water passing by the probe. The circulation period of the test basin was on the order of 1 min when paddling at full speed.

We shifted the probe around during pilot studies and found that one point near the inlet of the aerator provided a consistent and representative sample of average tank conditions. Observations from the left side of Fig. 2 produced erratic measurements, as saturated turbulent jets emanating from the paddles created eddies intertwined with oxygen deficient water from upstream. Oxygen readings were more consistent at points (A, B, C, and D) on the right side of the tank. Only point D was used for on-going work because it was closer to the aerator intake and assumed to produce the best mix of tank water after dissipation of turbulence, yet far enough away to avoid splash effects.

In another pilot study it was found that increasing depth of water column from 600 to 850 mm resulted in a increasing mass transfer effect of a particular aerator, but we were constrained by overflowing waves, as the basin was only 900 mm deep. For on-going tests the water filled to no more than 750 mm, specifically as recorded in Tables 1–3 Some water escaped with splashing at higher speeds, so the levels decreased until the tank was refilled. The tank was drained and water was replaced well before total dissolved solids accumulated to the 2 mg/l maximum concentration allowed in the standard (ASCE, 1993).

Three sets of experiments were conducted for each aerator, with incremental tests of performance while increasing the speed of A/C power supply to the motor: 30; 35; 37; 40; 42; 45; 50 Hz (paddling near 62; 73; 76; 82; 87; 93; 103 rpm). We plotted the increasing trend of each speed-control series, and report the mean and standard error of the three samples of data at each speed. The mean oxygen transfer rating

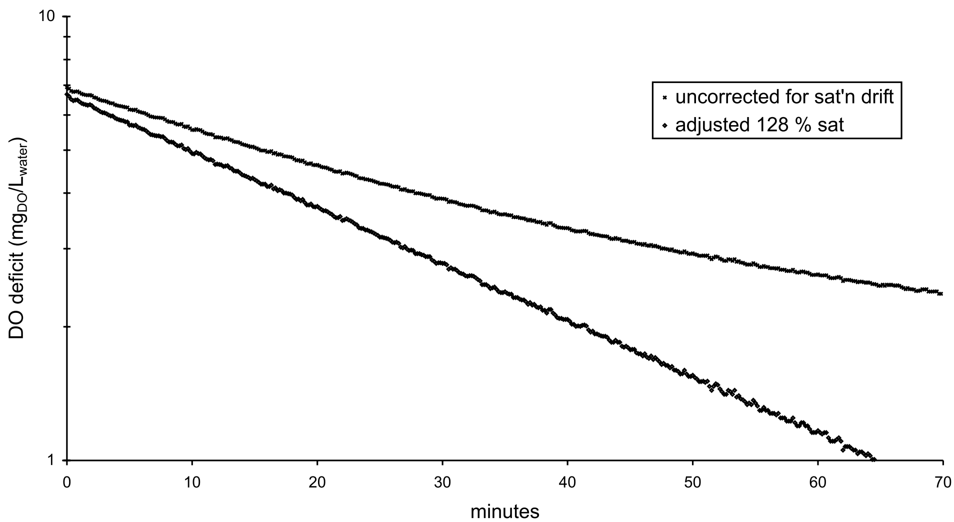

Fig. 3. Example DO deficit of paddlewheel A test #1 at 62 rpm speed. The shape of the plots depend on the estimation of saturation capacity C_s^*, from which DO measurements are referenced to determine DO-deficit. The plots should be linear when the DO-deficit is on a logarithmic scale, but raw data was non-linear (upper curve) because the estimation of C_s^* was incorrect. Least squares fit of the slope of the log of DO-deficit vs elapsed time (lower curve) determined re-aeration time-constant $(1/K_La)$.

Table 1
Observed performance of paddlewheel A

Time	Date	TDS (ppt)	Depth (cm)	Speed (rpm)	Power (kW)	C_s^+ Sat'n drift	R^2 of K_La	SOTR (kg_{DO}/h)	SAE (kg_{DO}/h)
11:17	7 Dec	0.13	74.5	62.4	0.400	128%	−1.000	0.314	0.786
13:01	7 Dec	0.19	74.5	72.4	0.540	128%	−1.000	0.494	0.915
14:12	7 Dec	0.25	74.5	76.5	0.577	128%	−1.000	0.576	0.999
15:27	7 Dec	0.30	74.5	82.5	0.670	127%	−0.999	0.690	1.030
10:03	8 Dec	0.37	73.5	86.7	0.700	111%	−0.998	0.831	1.188
11:02	8 Dec	0.43	73.5	92.7	0.773	109%	−0.998	0.885	1.145
12:14	8 Dec	0.48	73.5	102.9	0.893	106%	−0.997	0.955	1.069
13:25	8 Dec	0.54	73.5	62.4	0.400	108%	−1.000	0.324	0.809
15:08	8 Dec	0.60	73.5	72.4	0.540	110%	−0.999	0.508	0.941
16:35	8 Dec	0.65	73.5	76.5	0.577	109%	−0.999	0.573	0.993
9:30	11 Dec	0.71	73.0	82.5	0.670	118%	−0.999	0.738	1.102
10:35	11 Dec	0.77	73.0	86.7	0.700	118%	−0.999	0.814	1.163
11:42	11 Dec	0.83	73.0	92.7	0.773	118%	−0.999	0.891	1.152
12:50	11 Dec	0.89	73.0	102.9	0.893	118%	−0.999	0.973	1.089
13:47	11 Dec	0.94	74.5	62.4	0.400	121%	−1.000	0.353	0.882
15:32	11 Dec	1.00	74.5	72.4	0.540	120%	−0.999	0.549	1.016
16:45	11 Dec	1.06	74.5	76.5	0.577	118%	−0.999	0.625	1.083
9:31	12 Dec	1.11	74.5	82.5	0.670	104%	−0.998	0.778	1.162
10:39	12 Dec	1.17	73.5	86.7	0.700	104%	−0.998	0.844	1.206
12:06	12 Dec	1.22	73.5	92.7	0.773	105%	−0.998	0.971	1.255
13:13	12 Dec	1.27	73.5	102.9	0.893	106%	−0.996	1.134	1.270

Note: C_s^+ (Sat'n drift) is the factor that was applied to oxygen saturation measurements so that re-aeration trend would asymptotically approach an effective value of C_s^*. R^2 is the correlation coefficient of least squares fit of the time-constant of re-aeration. SOTR and SAE are the Standard oxygen transfer rate and Standard aeration efficiency, respectively.

Table 2
Observed performance of paddlewheel B

Time	Date	TDS (ppt)	Depth (cm)	Speed (rpm)	Power (kW)	C_s^+ Sat'n drift	R^2 of K_La	SOTR (kg_{DO}/h)	SAE (kg_{DO}/h)
9:38	14 Dec	0.11	74.5	62.4	0.403	106%	−1.000	0.339	0.840
11:43	14 Dec	0.17	74.5	72.4	0.553	109%	−0.999	0.559	1.010
13:04	14 Dec	0.23	74.5	76.4	0.613	109%	−0.999	0.632	1.030
14:46	14 Dec	0.29	74.5	82.4	0.703	110%	−0.999	0.769	1.093
15:44	14 Dec	0.34	73.5	86.5	0.743	109%	−0.999	0.831	1.117
16:59	14 Dec	0.48	73.5	92.5	0.830	108%	−0.998	0.915	1.103
10:36	15 Dec	0.46	73.5	102.5	0.970	115%	−0.998	1.056	1.089
12:20	15 Dec	0.52	68.5	62.4	0.403	115%	−1.000	0.302	0.750
14:40	15 Dec	0.58	68.5	72.4	0.553	115%	−0.999	0.464	0.839
11:32	18 Dec	0.63	69.0	76.4	0.613	112%	−0.999	0.466	0.760
12:47	18 Dec	0.70	69.0	82.4	0.703	112%	−0.999	0.544	0.773
15:05	18 Dec	0.76	69.0	86.5	0.743	110%	−0.999	0.565	0.760
16:28	18 Dec	0.80	69.0	92.5	0.830	113%	−0.999	0.677	0.815
10:00	19 Dec	0.84	69.0	102.5	0.970	103%	−0.998	0.688	0.709
11:58	19 Dec	0.92	69.0	62.4	0.403	110%	−0.999	0.364	0.902
13:39	19 Dec	1.00	69.0	72.4	0.553	110%	−0.999	0.421	0.760
15:15	19 Dec	1.03	69.0	76.4	0.613	110%	−0.999	0.509	0.830
16:24	19 Dec	1.05	69.0	82.4	0.703	111%	−0.999	0.574	0.817
10:23	20 Dec	1.07	68.5	86.5	0.743	110%	−1.000	0.440	0.591
11:45	20 Dec	1.12	68.5	92.5	0.830	112%	−0.999	0.681	0.821
12:49	20 Dec	1.16	68.5	102.5	0.970	113%	−0.998	0.782	0.806

Note: C_s^+ (Sat'n drift) is the factor that was applied to oxygen saturation measurements so that re-aeration trend would asymptotically approach an effective value of C_s^*. R^2 is the correlation coefficient of least squares fit of the time-constant of re-aeration. SOTR and SAE are the Standard oxygen transfer rate and Standard aeration efficiency, respectively.

Table 3
Observed performance of paddlewheel C

Time	Date	TDS (ppt)	Depth (cm)	Speed (rpm)	Power (kW)	C_s^+ Sat'n drift	R^2 of K_La	SOTR (kg_{DO}/h)	SAE (kg_{DO}/h)
9:27	30 Nov	0.2	69.0	62.0	0.473	108%	−0.999	0.381	0.805
11:09	30 Nov	0.18	69.0	72.0	0.633	108%	−0.999	0.598	0.944
12:08	30 Nov	0.22	69.0	76.0	0.693	109%	−0.999	0.682	0.983
13:23	30 Nov	0.26	69.0	82.0	0.783	110%	−0.998	0.861	1.099
15:08	30 Nov	0.31	69.0	86.0	0.837	109%	−0.997	0.944	1.129
16:02	30 Nov	0.38	69.0	92.0	0.933	108%	−0.995	0.988	1.059
10:11	1 Dec	0.66	68.5	102.0	1.073	108%	−0.995	1.247	1.162
11:12	1 Dec	0.70	68.5	62.0	0.473	109%	−0.999	0.388	0.819
13:01	1 Dec	0.78	68.5	72.0	0.633	107%	−0.999	0.581	0.916
15:29	1 Dec	0.85	68.5	76.0	0.693	109%	−0.999	0.665	0.959
17:00	1 Dec	0.93	68.5	82.0	0.783	111%	−0.999	0.789	1.007
9:25	4 Dec	1.01	67.5	86.0	0.837	106%	−0.997	0.902	1.078
10:26	4 Dec	1.06	67.5	92.0	0.933	108%	−0.996	1.095	1.174
11:48	4 Dec	1.11	67.5	102.0	1.073	109%	−0.996	1.334	1.243
13:20	4 Dec	0.79	67.5	62.0	0.473	109%	−0.999	0.396	0.837
16:25	4 Dec	1.08	67.0	72.0	0.633	110%	−0.998	0.623	0.982
11:13	5 Dec	1.15	66.5	76.0	0.693	105%	−0.998	0.706	1.018
9:09	6 Dec	1.65	66.5	82.0	0.783	121%	−0.999	0.867	1.107
10:34	6 Dec	1.68	66.5	86.0	0.837	121%	−0.999	0.939	1.122
12:42	6 Dec	1.83	66.5	92.0	0.933	122%	−0.998	1.035	1.109
14:26	6 Dec	1.75	66.5	102.0	1.073	123%	−0.998	1.219	1.136

Note: C_s^+ (Sat'n drift) is the factor that was applied to oxygen saturation measurements so that re-aeration trend would asymptotically approach an effective value of C_s^*. R^2 is the correlation coefficient of least squares fit of the time-constant of re-aeration. SOTR and SAE are the Standard oxygen transfer rate and Standard aeration efficiency, respectively.

was tabulated for each aerator and at each speed, based upon the three tests. These were then sorted in ascending order. The data were analysed using one-tailed paired t-tests, to determine significance posing the hypothesis that the performance at one speed would be greater than the performance at another speed. The one-tailed test is appropriate because we have hypothesised an increase in performance (Zarr, 1999).

3. Results

The power demand of each of the three paddlewheels are presented in Fig. 1, indicating that load increases with a power of about 1.6, with the implication that half-speed operation demands one-third of the power as running at full speed.

Oxygen transfer measurements required analysis, initiated with observation of oxygen scavenger. Observed log[DO deficit] was plotted in Fig. 3 as an example of the process. The R^2 provides a measure of the goodness of fitting a straight line to the rate of re-saturation of oxygen in each test. As anticipated in commentary C of ASCE (1993), the apparent saturation condition C_s^* of the tank solution drifted in the course of testing. Saturation condition was corrected by a factor C_s^+, determined by using a spreadsheet solver algorithm to optimise the goodness of fit. SOTR was derived from the slope of the curve, corrected for temperature, and then divided by power demand to determine SAE. Tables 1–3 report data and re-aeration analysis.

The mean values of the SOTR's and SAE's of the aerators tested are summarised in Table 4 for full speed operation, with 50 cycles/s alternating power. These means were based on a sample size of three in each case. Means and standard deviations of these samples were assumed to follow a normal distribution to generate the curves in Fig. 4 to illustrate that a one-tailed significance test is appropriate to compare increasing performance with speed. One-tailed t-test significance was applied with a 95% confidence level, as tabulated in Table 5.

Figs. 5–7 represent paddlewheel A, B, and C performance, respectively. Datapoints of individual observations are denoted with solid symbols. Open square symbols and error bars show the mean and standard error of the triplicate-set of observations at each speed.

Fig. 8 is a photograph of paddlewheel 'A' operating at breakpoint speed 76 rpm, which shows the trajectory of water droplets generally move downstream (right to left). Fig. 9 is a photograph of paddlewheel 'A' operating at normal full speed 103 rpm, showing typical widespread spray in all directions, including retrograde 'backsplash'.

4. Discussion

Paddlewheel blades rotated between 102 and 103 rpm when electric power A/C was fixed at 50 cycles/s, as determined by the 14:1 gearbox and the 4-pole motor.

Table 4
Average performance of paddlewheel aerators operating at full speed (paddling 102 rpm with 50 Hz A/C power), based on three tests each

	Water depth (cm)	Mean SOTR (kg/h)	Std Err SOTR (kg/h)	Power demand (kW)	Mean SAE (kg/kW h)	Std Err SAE (kg/kW h)
Paddlewheel A	74	1.020	±0.057	0.89	1.142	±0.064
Paddlewheel B	69	0.842	±0.111	0.97	0.868	±0.114
Paddlewheel C	69	1.267	±0.035	1.07	1.180	±0.032

Table 5
Aerator and speed sorted by relatively increasing mean SOTR and compared for significant differences

0.33	0.33	0.39	0.48	0.52	0.54	0.59	0.60	0.61	0.63	0.68	0.74	0.76	0.83	0.84	0.84	0.92	0.93	1.0	1.0	1.3	SOTR	
62	62	62	72	72	76	77	72	86	82	76	83	92	87	82	103	93	86	103	92	102		Speed
A	B	C	B	A	B	A	C	B	B	C	A	B	A	C	B	A	C	A	C	C	Aerator	
–		*	*	*	*	*	*		*	*	*	*	*	*	*	*	*	*	*	*	A	62
	–	*	*	*	*	*	*		*	*	*	*	*	*	*	*	*	*	*	*	B	62
		–		*		*	*		*	*	*	*	*	*	*	*	*	*	*	*	C	62
			–						*	*	*	*	*	*	*	*	*	*	*	*	B	72
				–		*	*			*	*		*	*		*	*	*	*	*	A	72
					–				*	*		*	*	*	*	*	*	*	*	*	B	76
						–				*	*		*	*		*	*	*	*	*	A	77
							–			*	*		*	*		*	*	*	*	*	C	72
								–				*			*				*	*	B	86
									–			*		*	*	*	*	*	*	*	B	82
										–			*	*		*	*	*	*	*	C	76
											–		*	*		*	*	*	*	*	A	83
												–								*	B	92
													–			*	*	*	*	*	A	87
														–		*	*	*	*	*	C	82
															–					*	B	103
																–		*	*	*	A	93
																	–			*	C	86
																		–		*	A	103
																			–	*	C	92
																				–	C	102

* denotes significant difference with one-tail t-test, $P<0.05$.

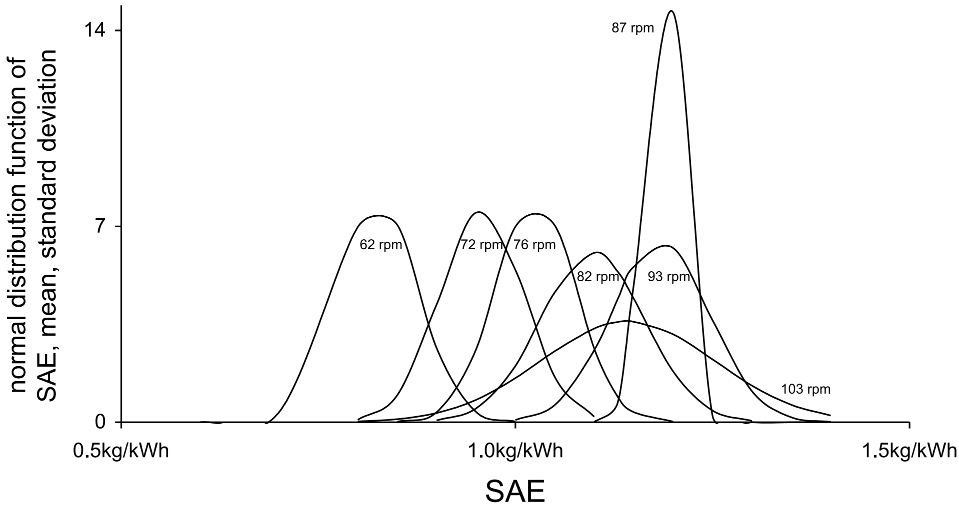

Fig. 4. Normal distributions of observations of paddlewheel A at various speeds. This figure establishes that a one-tailed significance test is appropriate for comparison of results as speed was increased. This also illustrates the variable confidence of estimated means, whereby 103 rpm is most undetermined, suggesting instability at this speed.

Note that the motor was nominally rated at 50 Hz A/C to run 1440 rpm. We adopt the null hypothesis and must say there is no proof that paddlewheel A performed better than B, although the standard errors of Table 4 do not quite overlap. The null hypothesis is strictly adopted because t-tests of Table 5 show no significant difference. Conversely, all indications are that there certainly is a significant improvement in SOTR comparing paddlewheel C to either of paddlewheels A or B operating at full speed.

Adjusting the frequency of A/C power effectively controlled the paddlewheel speed and resulted in significant differences in SOTR performance as tabulated in Table 5. There was generally an increase in oxygen transfer rate with speed, but paddlewheel A displayed a most distinct bump when paddling was increased from 76 to 82 rpm. This particular aerator was most efficient paddling at 87 rpm, with an apparent drop as paddling increased to 103 rpm (50 Hz A/C).

It is hypothesised in the present paper that paddlewheels work better when backsplash is avoided, which was visually observed when running faster than 76 rpm. Backsplash could be avoided by A/C frequency control or by fitting an 18:1 gearbox instead of the standard 14:1. It is believed that backsplashing caused paddlewheels A and C to display a flattening of the SAE performance curves above 76 rpm.

Paddlewheels B also increased oxygen transfer rate with speed, but efficiency did not display a significant trend. Perhaps this particular model reduced the backsplash effect when operating above the critical speed. Perhaps the elastic behaviour of paddlewheels A, B, and C are somehow different to such an extent that droplets are flicked off in different ways. But it is the opinion of the authors that some experimental error caused paddlewheel B to behave strangely, especially during test # 3 at 87 rpm.

The rotational speed of a paddlewheel, rpm, and the tip-speed, V (m/s) of the paddles are related in Eq. (6), based on wheel diameter, D.

$$V = \frac{\mathrm{rpm}\pi D}{(60\ \mathrm{s/min})} \tag{6}$$

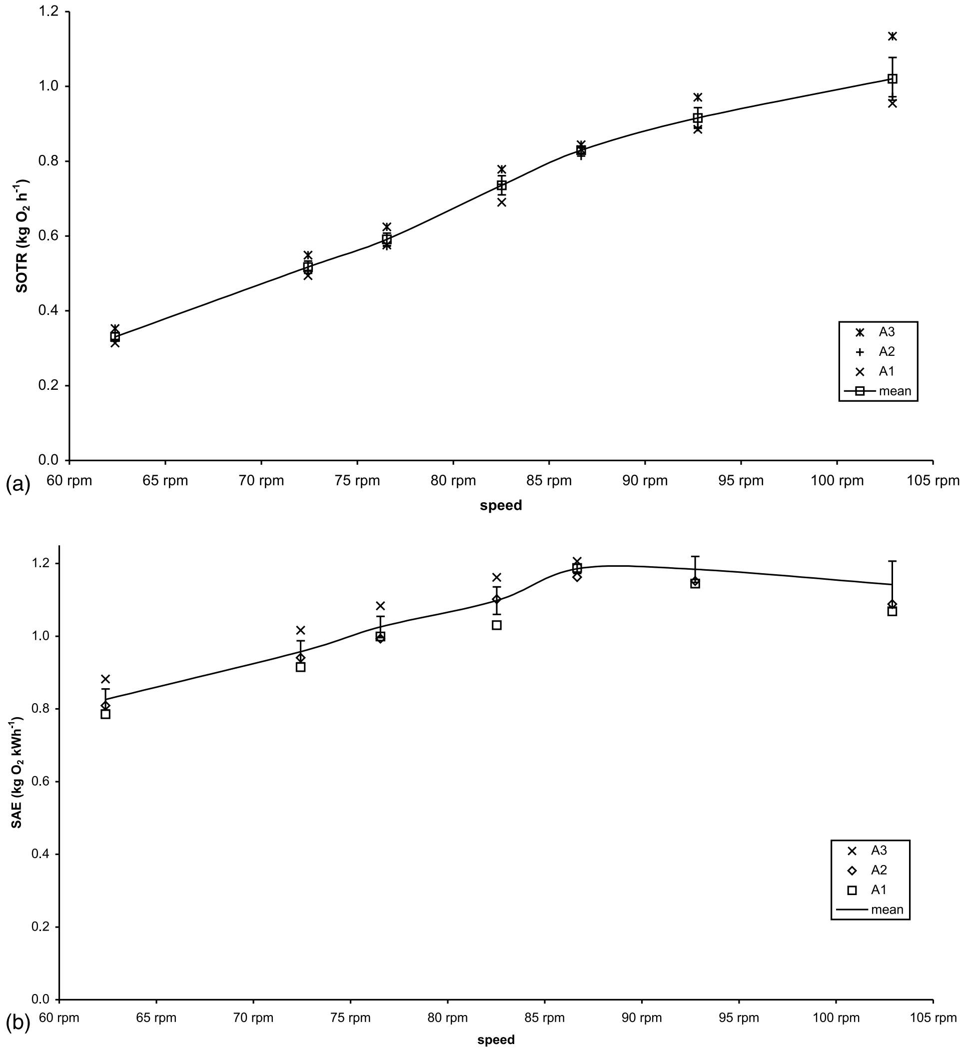

Fig. 5. Paddlewheel A results from oval basin filled to 740 mm. (a) Standard oxygen transfer rate (SOTR). (b) Standard aerator efficiency (SAE).

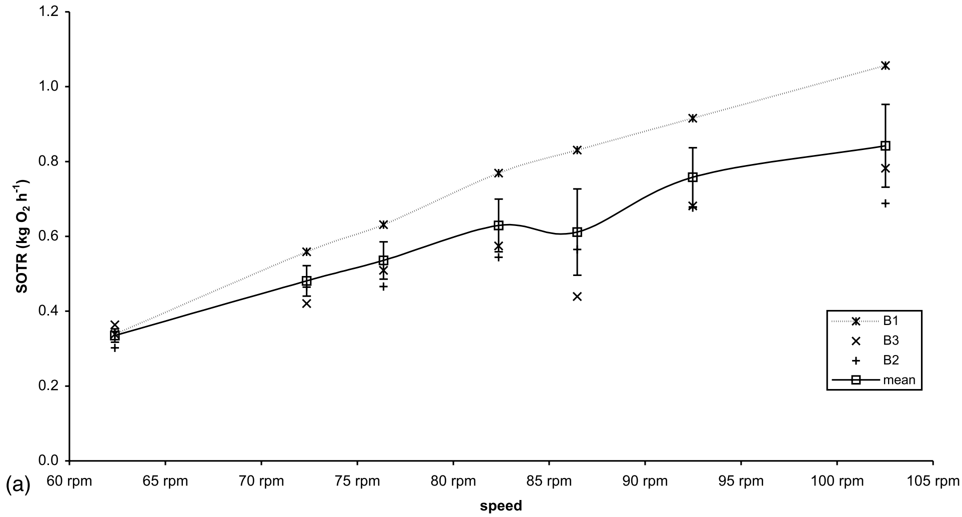

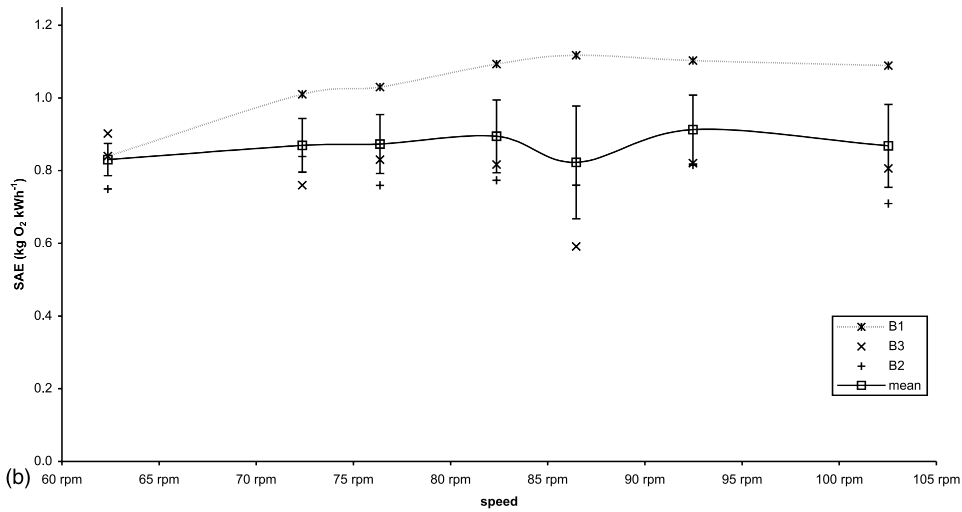

Fig. 6. Paddlewheel B results from oval basin filled to 690 mm. (a) Standard oxygen transfer rate (SOTR). (b) Standard aerator efficiency (SAE).

We now suggest in this discussion that backsplashing should be expected when the potential energy (mgh) equals the kinetic-energy ($\frac{1}{2}mV^2$): where m is the mass of water handled by the aerator blades; h is the height that water is tossed. From all of the forgoing, Eq. (7) has been written for the unique breakpoint (bp) condition at the transition between desirable operation and unintentional backsplashing.

$$\mathrm{rpm}_{\mathrm{bp}} = \frac{60\ \mathrm{rpm/Hz}}{\pi} \frac{\sqrt{g \times h_{\mathrm{bp}}}}{D} \tag{7}$$

Undesirable backsplash droplets fly off a paddlewheel in a retrograde trajectory, and the wheel imparts such motion only above the axis of rotation. Spray is directed correctly where droplets fly off the wheel before being carried above the height of the axis of rotation. For this reason it is believed that the backsplash breakpoint height, h_{bp}, is close to half the wheel diameter, $(\frac{1}{2})D = R$, which is the wheel radius. So the backsplash breakpoint speed, $\mathrm{rpm}_{\mathrm{bp}}$, is predicted with Eq. (8).

$$\mathrm{rpm}_{\mathrm{bp}} = \frac{60\ \mathrm{rpm/Hz}}{\pi}\sqrt{\frac{g}{D}} \tag{8}$$

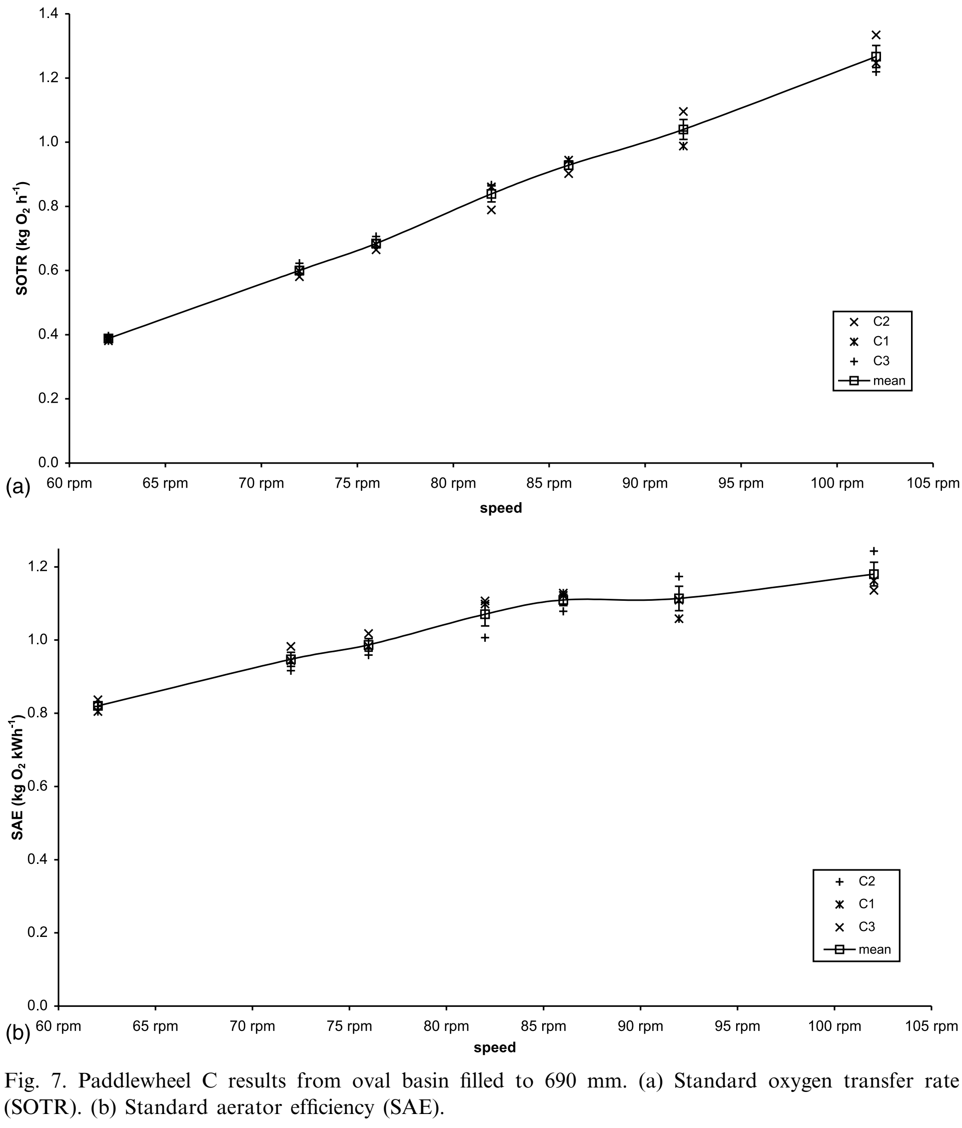

Fig. 7. Paddlewheel C results from oval basin filled to 690 mm. (a) Standard oxygen transfer rate (SOTR). (b) Standard aerator efficiency (SAE).

Fig. 8. Photograph of paddlewheel A operating below breakpoint speed (77 rpm).

For the 680-mm paddlewheels studied in the present paper the predicted breakpoint speed is 72 rpm (36 Hz A/C power into the motor). Boyd (1998) found the best results for his spiral paddlewheel were obtained with the larger wheel (91 cm) and at the lower end of his experimental range, at a speed of 75 rpm. These conditions indicate the tip-speed kinetic energy was 65 cm head of water column, which was nearly equivalent to his prototype paddlewheel radius. It appears that his best results were obtained when operating near the backsplash breakpoint condition, but no photographic evidence was available in his paper.

Paddlewheel aerators tested in our experiments would have earned better SAE ratings if they had more efficient gearboxes. This is asserted because less motor capacity would have been used to deliver mechanical power to the paddles. The three paddlewheels that we tested were similar in design, with a vertical motor/gearbox assembly under a central enclosure. The gearboxes were all worm-driven, with wear reported by most Australian aquaculturalists. Reduced speed operation certainly reduces wear and tear of the aerator, but also reduces erosion of pond banks and improves pond sediment condition (Peterson and Indran, 2001).

Some discussion of electric power savings is appropriate at this point. A substantial amount of energy can be saved through active control of electric power frequency (Peterson and Pearson, 2000; Peterson and Indran, 2001). The results of

Fig. 9. Photograph of paddlewheel A operating at normal full speed (103 rpm).

the present paper allow the farmer to estimate the actual oxygen transfer of Taiwanese paddlewheels if the level of oxygen saturation is known. Working aquaculture ponds are dominated by algal blooms, where DO generally becomes saturated during daylight. Actual oxygen transfer from an aerator will be negative whenever pond water oxygen is above the saturation level. At such times the speed of aeration should be reduced to control SOTR to as low a value as practical without stalling out motors or loosing effective pond circulation. Good results were obtained when speed was cut 2 h after sunrise and full speed operation was resumed at sunset (Peterson and Indran, 2001; Peterson, 2001). In another trial of several ponds stocked with marine shrimp, it was decided to delay 2 h after sunset before switching back to full speed, with no adverse effect (Peterson and Berry, unpublished). Electrical harmonics make it difficult to control many ponds with a single variable frequency inverter (Nesbitt, 2000).

The relationship of DO saturation and temperature are established for freshwater (Battino and Clever, 1966; Benson and Krause, 1980). Salinity adds another dimension (Benson and Parker, 1961; Colt, 1984; Garcia and Gordan, 1992) which effects solubility. Perhaps not as accurate as later models, Eq. (9) (Weiss, 1970) simply estimates DO mL_{DO}/L_{water} given T degrees K (273.15 + °C) and S salinity in ppt as follows:

$$\ln(\mathrm{DO}) = A1 + A2(100/T) + A3\ln(T/100) + S[B1 + B2(T/100) + B3(T/100)^2] \quad (9)$$

where coefficients $A1 = -173.4292$; $A2 = 249.6339$; $A3 = 143.3483$; $A4 = -21.8492$; and salinity terms $Bl = -0.033096$; $B2 = 0.014259$; $B3 = -0.001700$. Since the density of oxygen in an aqueous solution is about 0.7 kg/m^3, then the units of DO ($mL_{\mathrm{DO}}/L_{\mathrm{water}}$) may be divided by 0.7 to estimate oxygen concentration C_s^*, expressed as $\mathrm{mg_{DO}}/L_{\mathrm{water}}$. Aquaculturalists may estimate % saturation by dividing concentration readings by C_s^*. The central theme is that aeration is not required if DO is above 100% sat.

5. Conclusions

The rotational speed of a paddlewheel is a significant factor affecting the performance of the machine as an aerator. Of particular note is the observation of backsplashing when kinetic energy (pumping head) is greater than the radius of the wheel. It appears that backsplashing dilutes the oxygen-starved water entering the paddlewheel, thereby degrading the operational efficiency. An equation is proposed to predict the breakpoint frequency, $\mathrm{rpm_{bp}} = (60\ \mathrm{rpm/Hz/p})(g/D)^{1/2}$. Aerator users and manufacturers are advised to reduce the nominal operational speed of paddlewheel aerators so that the breakpoint speed is not exceeded. Such may be achieved by replacement of the mechanical gears with a lower ratio, or by actively controlling speed with a variable frequency drive (VFD inverter).

Acknowledgements

The present research paper was made possible with a salary provided by the Department of Civil and Environmental Engineering, James Cook University under the Kevin Stark Research Fellowship. The Aquaculture CRC and James Cook University funded research infrastructure. Oxygen loggers, consumables, and wages for research assistance were funded from the Sustainable Industries Division, Environmental Protection Agency, Brisbane, Queensland. The variable frequency inverter was donated by CMG Drive Dynamics of Acadia Ridge, Queensland. Local aquaculture equipment suppliers loaned paddlewheels.

References

American Society of Civil Engineers (ASCE), 1993. Measurement of Oxygen Transfer in Clear Water. ANSI/ASCE-2-91, ANSI Approved June, 1992 second ed. ASCE, New York.

Battino, R., Clever, H.L., 1966. The solubility of gases in liquids. Chem. Rev. 66, 395–463.

Benson, B., Parker, P.D.M., 1961. Relations among the solubilities of nitrogen, argon and oxygen in distilled water and seawater. J. Phys. Chem. 65, 1489–1496.

Benson, B.B., Krause, D., 1980. The concentration isotopic fractionation of gases dissolved in freshwater in equilibrium with the atmosphere. Limnol. Oceanogr. 25, 662–671.

Boyd, C.E., 1998. Pond water aeration systems. Aquacult. Eng. 18, 9–40.

Busch, C.D., 1980. Water circulation for pond aeration and energy conservation. Proc. World Mariculture Soc. 11, 93–101.

Colt, J., 1984. Computation of dissolved gas concentrations in water as functions of temperature, salinity, and pressure. Am. Fish. Soc. Spec. Publ. 14.

Fast, A.W., Boyd, C.E., 1992. Water circulation, aeration and other management practices. In: Fast, A.W., Lester, J.L. (Eds.), Marine Shrimp Culture: Principles and Practices. Elsevier, Amsterdam, pp. 457–495.

Fast, A.W., 1992. Penaeid grow out systems: an overview. In: Fast, A.W., Lester, L.J. (Eds.), Marine Shrimp Culture: Principles and Practices. Elsevier, Amsterdam, Netherlands.

Fast, A.W., Tan, E.C., Stevens, D.F., Olson, J.C., Qin, J., Barclay, D.K., 1999. Paddlewheel aerator oxygen transfer efficiencies at three salinities. Aquacult. Eng. 19, 99–103.

Garcia, H.E., Gordan, L.I., 1992. Oxygen solubility in seawater: better fitting equations. Limnol. Oceanogr. 37 (6), 1307–1312.

Gnezdiloff, L.K., 1999. Modelling of dissolved oxygen from an aerator. Bachelor of Engineering Thesis, James Cook University of North Queensland, Townsville, Australia.

Lewis, W.K., Whitman, W.C., 1924. Principles of gas absorption. Ind. Eng. Chem. 16, 1215.

Nesbitt, P., 2000. Study of Variable Frequency Drives in Aquaculture. Bachelor of Engineering (Electrical) Thesis, James Cook University of North Queensland, Townsville, Australia.

Peterson, E.L., 1997. Pond aeration study. Queensland Aquaculture News 11, 4–5. Department of Primary Industries, Bribie Island, Queensland, Australia.

Peterson, E.L., 2001. Review of engineering for sustainable shrimp farming. In: Browdy, C.L., Jory, D.E. (Eds.), The New Wave, Proceedings of the Special Session on Sustainable Shrimp Farming, Aquaculture 2001. The World Aquaculture Society, Baton Rouge, Louisiana, USA, pp. 153–167.

Peterson, E.L., Patterson, J.C., 1999. Speed control of mechanical aerators. In: Stafford, C. (ed.) Proceeding of the Prawn Farmers Workshop Held at DPI South Johnstone 20–21 October 1999, DPI Northern Fisheries Centre, Cairns, pp. 45–47. ISSN 0728-067X. Agdex 477/10.

Peterson, E.L., Patterson, J.C., 2000. Energy Auditing Aquaculture Facilities. In: 3rd Queensland Environmental Conference-Sustainable Environmental Solutions for Industry and Government, 25 and 26 May 2000, Brisbane, pp. 177–181.

Peterson, E.L., Pearson, D., 2000. Round peg in a square hole: aeration in a square shrimp pond. Global Aquacult. Advocate 3 (5), 44–46.

Peterson, E.L., Indran, G., 2001. Process control of pond sediment redox. In: World Aquaculture 2001 Book of Abstracts. World Aquaculture Society, Orlando, Florida, USA.

Rogers, G.L., 1989. Aeration and circulation for effective aquaculture pond management. Aquacult. Eng. 8, 349–355.

Weiss, R.F., 1970. Solubility of nitrogen oxygen and argon in water and seawater. Deep-Sea Res. 17, 721–735.

Zarr, J.H., 1999. Biostatistical Analysis. Prentice Hall.